PHYSICAL REVIEW A **75**, 033408 (2007)

Routes to multiphoton double ionization in combined extreme ultraviolet and infrared laser pulses

M. Böttcher,[1] H. Rottke,[1] N. Zhavoronkov,[1] W. Sandner,[1] P. Agostini,[2,3] M. Gisselbrecht,[3] and A. Huetz[3]
[1]*Max-Born-Institute, Max-Born-Straße 2A, D-12489 Berlin, Germany*
[2]*Department of Physics, Ohio State University, Columbus, Ohio 43210, USA*
[3]*LIXAM (UMR 8624), Batiment 350, Centre d'Orsay, 91405 Orsay Cedex, France*
(Received 30 May 2006; published 21 March 2007)

Xenon multiphoton double ionization pathways are studied in a reaction microscope using a pump-probe arrangement of extreme ultraviolet high harmonic and infrared laser radiation. The momentum of photoelectrons is recorded in coincidence with singly or doubly charged ions. Among all possible routes to multiphoton double ionization, sequential processes using ionic excited states as intermediate steps are clearly identified.

DOI: 10.1103/PhysRevA.75.033408 PACS number(s): 32.80.Rm, 32.80.Fb, 32.80.Wr

Photoionization is a fundamental quantum physics process and one of the basic tools giving access to structural and dynamical properties of atoms. Depending on the light frequency and intensity, it can result in the ejection of *two* valence shell electrons from a variety of mechanisms. (i) Following the absorption of a single high-energy photon: photo double ionization (DI) is governed by electron correlation. It is most intensively studied for that property [1,2]. (ii) Through multiphoton absorption: DI can occur in a low-frequency, intense (10^{12} W/cm^2) laser beam. Multiphoton DI (MPDI) was discovered in the mid-1970s [3] and investigated by several groups [4]. (iii) In an electric-field mediated three-step process at even higher light intensity (10^{15} W/cm^2) [5]. This "strong field" DI was the object of tremendous interest during the past decade [6] and the tag "nonsequential DI," as opposed to a sequence of two independent field ionization processes, is attached to it. Despite a long history, little is known about low-order N-photon DI. Experimental constraints restricted most studies to orders $N \geqslant 8$ for which a perturbation analysis is already intractable [4]. Although laser advances have stimulated new theoretical [7,8] and experimental [9] studies of two-photon DI of helium, experiments have been limited so far to the investigation of total ionization yields. Nevertheless, a complete analysis of helium two-photon DI seems possible in the near future, as intense extreme ultraviolet (XUV) sources with high enough repetition rates become available. This will undoubtedly be a considerable breakthrough and will provide new insights into the underlying three-body problem. Meanwhile, the superposition of XUV and IR laser pulses which can be achieved with synchrotron sources [10], or high harmonic generation, approach this goal. Combining this technique with a reaction microscope [11] is the object of the present work.

This paper describes the investigation of few-photon DI of xenon, chosen because of its relatively low ionization potentials, which are adapted to the current possibilities of high harmonic sources, although the large Xe mass limits the reaction microscope capabilities to the precise extraction of only one electron momentum. The intensity of the harmonic source allows us to study DI pathways which involve one XUV photon and one or several infrared photons. The pathways reaching the double continuum final state of xenon fall into two categories "nonsequential" and "sequential." The nonsequential direct DI mechanism [Fig. 1(a)] results in the simultaneous emission of two electrons with a continuous energy spectrum. The nonsequential indirect one is a stepwise process: a first electron is emitted and a second one is excited to a Rydberg state which autoionizes with some delay. The energy spectrum is discrete and one component (E_2) does not depend on the photon energies. On the "sequential" route [Fig. 1(b)] the relay state is an ionic excited state below the double ionization threshold. By selecting XUV photon energies lower than that threshold, the absorption of at least one infrared photon is required for double ionization.

The setup [11] and the reaction microscope [12] have been extensively described. Briefly, high harmonics are generated from the 4.5 mJ, 45 fs pulses of a Ti:sapphire laser system at 810 nm at a repetition rate of 1 kHz [13]. A monochromator (toroidal mirror and flat-field grating) is used to select a single harmonic (bandwidth: ≈150 meV) which crosses a supersonic Xe atomic beam in the reaction micro-

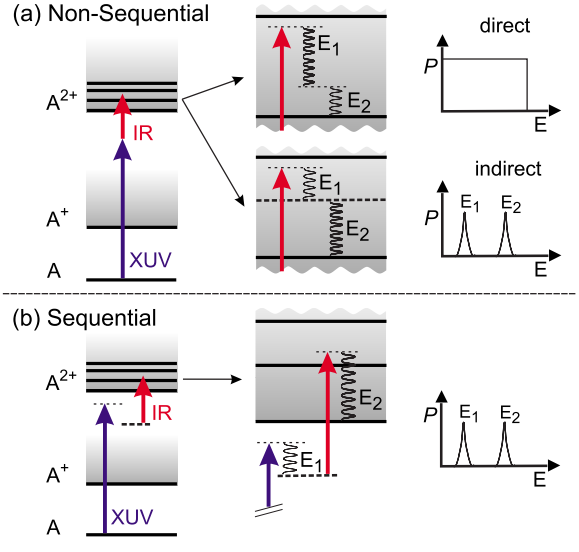

FIG. 1. (Color online) Pathways to multiphoton DI: (a) nonsequential "direct," or "indirect" through an A^{+*} Rydberg state (thick dashed line). (b) Sequential: via an A^{+*} state below the DI continuum threshold. Corresponding photoelectron spectra are schematized on the right.

scope, 2 m downstream from the harmonic source [11]. We concentrate here on results gained with the 17th and 21st harmonics at wavelengths 47.65 nm ($\hbar\omega$=26.02 eV) and 38.57 nm ($\hbar\omega$=32.14 eV) respectively, selected by a monochromator which stretches the harmonic pulses (initial pulse width: 10–20 fs) to 3.0±0.5 ps. Photoions are extracted by a small homogeneous electric field (3.3 V/cm) pointing towards the ion detector and coinciding with the direction of polarization of the laser beams. At the end of a field-free drift space, the ions hit a position-sensitive microchannel-plate detector. The same electric field guides the electrons in the opposite direction to a second position-sensitive detector. A small fraction of the Ti:sapphire pump beam, reflected from a beam splitter, is steered into the microscope chamber through a rear window, reflected back on a mirror and eventually superposed on the harmonic beam at a small angle at the point of intersection with the supersonic Xe beam. In order to minimize the temporal mismatch between the XUV (3.0±0.5 ps) and infrared (45 fs) pulses the latter are stretched to about 2.5 ps by passing them through 65 mm of SF-10 glass. The dispersion in the image plane of the monochromator puts a lower limit on the spot size of the harmonic beam in the interaction region (≈0.5 mm in the dispersion plane). To achieve maximum MPDI, the infrared beam had to be adapted to this beam size. The maximum infrared intensity in the overlap region is therefore rather low, as confirmed by the absence of sizable sidebands in the photoelectron spectrum around the 21st harmonic line, a signature of the two-color photoionization:

$$\mathrm{Xe} + \hbar\omega_{H21} \pm n\hbar\omega_{IR} \rightarrow \mathrm{Xe}^{+} + e(E_{kin}) \tag{1}$$

with E_{kin}=20.01 eV±n1.53 eV. This puts an upper limit of 1.2×10^{11} W/cm^2 to the effective infrared intensity. Photoelectron spectra are taken in coincidence with singly or doubly charged ions, respectively. The photoelectron momentum is recovered with a resolution of ≈0.02 a.u. In order to minimize false coincidences, the photoelectron count rate is kept well below the laser pulse repetition rate.

We first discuss the case of the 21st harmonic. The double ionization threshold (Xe^{2+} ground state) is split into ^3P (J=0,1,2), ^1D (J=2), and ^1S (J=0) states with a lowest energy of 33.1 eV above the Xe ground state [14]. Since the 21st harmonic has a photon energy of 32.14 eV, below that threshold, xenon must absorb at least one infrared photon (1.53 eV) in excess of one harmonic photon, to reach the lowest double ionization continuum. Angle-integrated photoelectron spectra recorded in coincidence with Xe^+ and Xe^{2+} ions, respectively, are shown in Fig. 2. The Xe^{2+} signal vanishes under irradiation with the 21st harmonic or infrared alone. In Fig. 3 the dependence of the ion yield ratio $[Xe^{2+}]/[Xe^+]$ on the delay $\tau=t_{IR}-t_{H21}$ between the infrared and 21st harmonic pulses is shown. If the infrared precedes the harmonic pulse ($\tau<-4$ ps) no MPDI is found. When the pulses start to overlap the ratio rises linearly for $-1<\tau<1$ ps and then stays constant from $\tau\approx2$ ps up to the maximum delay of 7 ps we used. This dependence obviously rules out any nonsequential MPDI (Fig. 1) for which the ratio should decrease back to zero when the infrared pulse

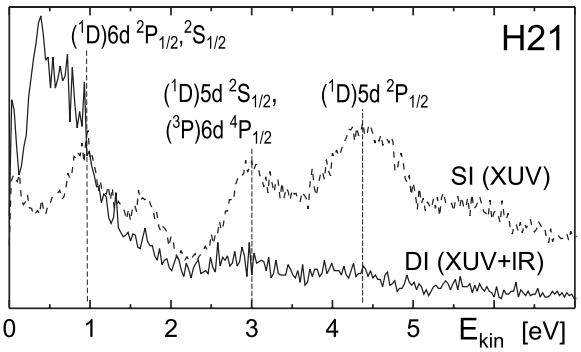

FIG. 2. Photoelectron spectra from SI by the 21st harmonic alone (dashed curve) and DI when superposed with the fundamental radiation (full curve). Xe $5s^15p^6$ correlation satellites are indicated by straight lines.

arrives after the harmonic pulse. Thus under our experimental conditions, only sequential pathways are observed. This may change at a higher infrared light intensity, i.e., a higher infrared excitation rate. The observed sequential MPDI [Fig. 1(b)] passes through long-lived excited Xe^+ states (with a radiation lifetime in the nsec regime) necessarily located in energy below the harmonic photon energy. The outlined DI scenario is confirmed by well-defined structures in the photoelectron spectrum in coincidence with Xe^+ ions [Fig. 2 SI)] in the energy range 2–7 eV which are also discernible in the MPDI trace (DI). The first XUV excitation step liberates an electron with kinetic energy:

$$E_1 = \hbar\omega_{\mathrm{H21}} - E[(\mathrm{Xe}^{+})^{*}]. \tag{2}$$

This step is followed by the absorption of a small number of infrared photons until eventually one of the double ionization thresholds $^3P_{2,1,0}$, $^1D_2$, $^1S_0$ is reached:

$$E_2 = E[(\mathrm{Xe}^{+})^{*}] + n\hbar\omega_{\mathrm{IR}} - E[\mathrm{Xe}^{++}_{\mathrm{fin.state}}]. \tag{3}$$

With $\hbar\omega_{\mathrm{IR}}$=1.53 eV it follows that, depending on the final Xe^{2+} state populated, up to n=4 infrared photons are needed. The absence of detectable above-threshold ionization in the second ionization step confirms that the number of infrared photons involved in MPDI is indeed small (the minimum number necessary to reach the respective threshold).

Excited Xe^+ states which may become populated after absorption of the XUV harmonic photon are tentatively identified in the single ionization spectrum (Fig. 2) using spectral line data from [15–17]. They turn out to be Xe^+ $5p^4nl$ cor-

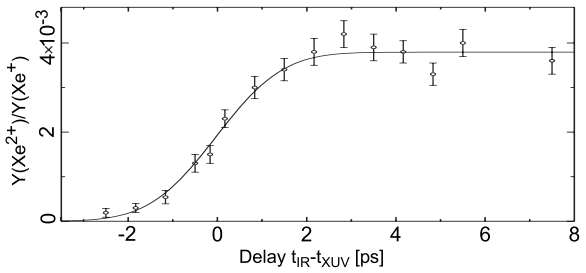

FIG. 3. The dependence of the ion yield ratio $[Xe^{2+}]/[Xe^+]$ on the delay of the infrared with respect to the 21st harmonic pulse.

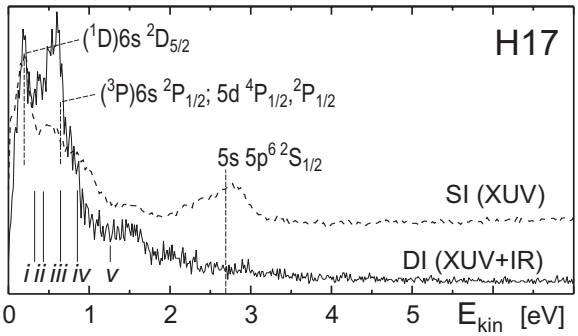

FIG. 4. Same as Fig. 2 with the 17th harmonic. The solid lines labeled (i)–(v) indicate photoelectron energies for multiphoton ionization of the Xe^+ $(^1D)6s(^2D_{5/2})$ state via the pathways: $+5\hbar\omega_{IR} \rightarrow Xe^{2+}$ $(^3P_2)$ (i); $+6\hbar\omega_{IR} \rightarrow Xe^{2+}$ $(^3P_1)$ (ii), and $(^3P_0)$ (iii); $+7\hbar\omega_{IR} \rightarrow Xe^{2+}$ $(^1D_2)$ (iv); $+8\hbar\omega_{IR} \rightarrow Xe^{2+}$ $(^1S_0)$ (v).

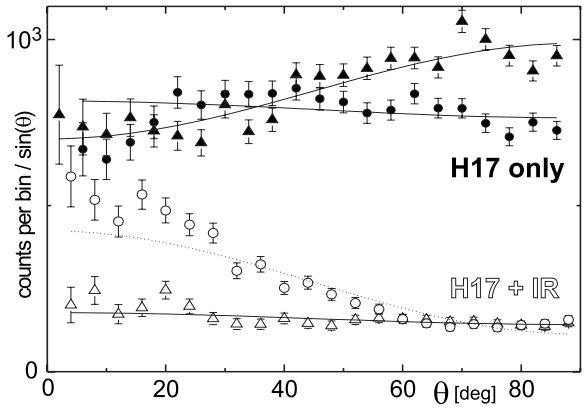

FIG. 5. Photoelectron angular distributions for DI (open symbols) and SI (filled symbols) by the 17th harmonic in the kinetic energy ranges 0.08–0.3 eV (triangles) and 0.45–0.75 eV (circles).

relation satellites which are well known in synchrotron spectroscopy. Only the position of states with the largest line strength measured at excitation wavelengths close to the one used here [15] are given. These line strengths depend critically on the excitation wavelength [15]. The significant XUV bandwidth does not allow a more precise identification of lines.

The above analysis can be tested by reducing the harmonic photon energy. Figure 4 shows typical spectra obtained with the 17th harmonic ($\hbar\omega$=26.02 eV). In this case the only remarkable structures in the single ionization spectrum correspond to the extraction of a 5*s* electron and to several close-by correlation satellites. However, the populated Xe^+ $5s^15p^6\ ^2S_{1/2}$ state does not contribute significantly to MPDI, as a corresponding structure is missing in the double ionization spectrum. This agrees with a small infrared multiphoton ionization probability of this state which requires the absorption of at least seven photons to reach the double ionization threshold. Moreover, such an ionizing transition to the Xe^{2+} $(5s)^2(5p)^4\ ^SL_J$ states involves the response of two electrons to the infrared light pulse, one electron filling the 5*s* hole while a second one is ejected.

For both harmonics, disentangling the MPDI photoelectron spectra in the energy range between 0 and $\hbar\omega_{IR}$ is a difficult task since several intermediate Xe^+ states and several close-lying ionization thresholds of the Xe^+ ion are involved. A partial analysis is given for the MPDI spectrum with the 17th harmonic in Fig. 4. One pronounced structure close to a kinetic energy of 0.2 eV appears in the single ionization spectrum (dashed line) as well as in the corresponding MPDI spectrum. It therefore may be assumed that the line in the MPDI spectrum predominantly also originates from the first Xe ionization step through the harmonic pulse. A candidate for the intermediate Xe^+ state populated on the line is $(^1D)6s\ ^2D_{5/2}$ [17]. A second pronounced line structure appears close to 0.6 eV where single ionization of Xe does not show a significant enhancement. Therefore multiphoton ionization of an intermediate Xe^+ state by the infrared light pulse can be expected to contribute predominantly to this structure. A reasonable assumption on the intermediate Xe^+ state is $(^1D)6s\ ^2D_{5/2}$ populated via the photoelectron line at 0.2 eV. Knowing the binding energy of this Xe^+ state and the energy of the accessible Xe^{2+} states with electron configuration $(5s)^2(5p)^4$ the possible kinetic energies of the photoelectrons from infrared multiphoton ionization can be determined. They are indicated by the lines beneath the spectrum in Fig. 4. The corresponding ionization pathways are given in the figure caption. The ones probably contributing to the MPDI line near 0.6 eV are six-photon ionization with final Xe^{2+} states (ii) $^3P_1$ and (iii) $^3P_0$.

The different physical nature of the two line structures in the MPDI spectrum in Fig. 4 near 0.2 eV [range (A)] and 0.6 eV [range (B)] becomes obvious in the angular distribution of the photoelectrons in Fig. 5. Angular distributions for single ionization of Xe by the harmonic light pulse and for the MPDI electrons are shown. For single ionization (SI) the angular distributions in both energy regions have quite small asymmetry parameters β=−0.22 (A) and β=0.04 (B). In the MPDI spectrum the angular distribution in region (B) is completely different. It becomes strongly peaked at an angle θ=0 with respect to the common polarization direction of the infrared and harmonic light pulses. Moreover, a simple asymmetry β parameter cannot be assigned to the angular distribution in region (B). Legendre polynomials with an order higher than 2 have to be introduced to fit this distribution. This underlines the multiphoton character of the transition giving rise to most of the photoelectrons in this line structure. The angular distribution of line (A) changes only little from single to double ionization. Within the error limits it can still be fitted with a Legendre polynomial of second order having a β parameter of 0.16. The only small change in β indicates that the MPDI electrons still mainly originate from the first Xe ionization step by the 17th harmonic with only a small contribution of electrons from the multiphoton ionization step of Xe^+.

In conclusion, a method to study low-order multiphoton DI pathways, photoelectron-photoion coincidence spectroscopy coupled to a table-top XUV high-order harmonic laser light source and infrared pulses, has been implemented and applied to xenon. Under our experimental conditions, only sequential MPDI routes have been clearly identified which involve the xenon correlation satellites $5s^25p^5nl^2L_J$ while the $5s^15p^6\ ^2S_{1/2}$ core-hole state which is closely related to the

satellites was found to play a negligible role. This, however, does not imply that nonsequential routes cannot be observed. One can speculate that higher-order harmonics or shorter pulses could enhance their probability. In addition, future experiments should give access to completely differential data with respect to the two photoelectrons and allow the isolation of weak nonsequential processes from the stronger sequential ones. The experimental method we used is general and flexible and it provides the possibility of choice of the relative polarization of the different colors. It can be extended either to the simpler and fundamental case of helium MPDI or to more complex systems like molecules and clusters with the possibility to exploit the full capabilities of a reaction microscope for low mass systems [12]. Nondispersive filtering of single or coherently superimposed groups of harmonic pulses will allow to use their natural pulse width in the femto- to attosecond time regime. This alone can increase their intensity by a factor of up to 1000 which may already open the possibility to get highly differential access to, for example, two-photon XUV alone processes. Helium two-photon DI would, after the single-photon case, be the simplest reaction with access to a two-photon three-body problem in a complete experiment. Such experiments should stimulate theoretical efforts in a completely new wavelength regime which is becoming accessible in nonlinear atomic and molecular dynamics investigations.

M.G. and A.H. acknowledge financial support by the EU (Contract No. RII3-CT-2003-506350, Laserlab Europe). P.A. thanks the Alexander von Humboldt Foundation for support.

[1] J. S. Briggs and V. Schmidt, J. Phys. B **33**, R1 (2000).
[2] L. Avaldi and A. Huetz, J. Phys. B **38**, 5861 (2005).
[3] V. V. Suran and I. P. Zapesochnyi, Pis'ma Zh. Tekh. Fiz. **1**, 973 (1975) [Sov. Tech. Phys. Lett. **1**, 420 (1975)].
[4] P. Lambropoulos, P. Maragakis, and Jian Zhang, Phys. Rep. **305**, 203 (1998).
[5] P. B. Corkum, Phys. Rev. Lett. **71**, 1994 (1993).
[6] A. Becker and F. H. Faisal, J. Phys. B **38**, R1 (2005).
[7] M. A. Kornberg and P. Lambropoulos, J. Phys. B **32**, L603 (1999).
[8] J. Colgan and M. S. Pindzola, Phys. Rev. Lett. **88**, 173002 (2002).
[9] Y. Nabekawa, H. Hasegawa, E. J. Takahashi, and K. Midorikawa, Phys. Rev. Lett. **94**, 043001 (2005).
[10] S. Aloise, P. O'Keeffe, D. Cubaynes, M. Meyer, and A. N. Grum-Grzhimailo, Phys. Rev. Lett. **94**, 223002 (2005).
[11] M. Böttcher *et al.*, J. Phys. B **38**, L389 (2005).
[12] J. Ullrich *et al.*, Rep. Prog. Phys. **66**, 1463 (2003).
[13] N. Zhavoronkov *et al.*, Appl. Phys. B: Lasers Opt. **79**, 663 (2004).
[14] J. H. D. Eland *et al.*, Phys. Rev. Lett. **90**, 053003 (2003).
[15] A. Fahlman, M. O. Krause, and T. A. Carlson, J. Phys. B **17**, L217 (1984).
[16] A. E. Slattery *et al.*, J. Phys. B **33**, 4833 (2000).
[17] A. Kikas *et al.*, J. Electron Spectrosc. Relat. Phenom. **77**, 241 (1996).